

Correlations in flux liquids with weak disorder

David R. Nelson and Pierre Le Doussal*

Lyman Laboratory of Physics, Harvard University, Cambridge, Massachusetts 02138

(Received 28 June 1990)

The response of an entangled flux liquid to a quenched random potential is studied. Dense flux liquids are stable to weak disorder and will persist even if the Abrikosov flux lattice is replaced by a vortex glass at low temperatures. Disorder produces "Lorentzian-squared" corrections to the vortex liquid structure function that may be detectable via neutron scattering. Our results are obtained by mapping the statistical mechanics of vortex lines onto the physics of disordered bosons in two dimensions and via a simpler hydrodynamic approach. A renormalization-group analysis shows that disorder does become relevant sufficiently close to H_{c1} , where it is no longer screened out by thermal fluctuations. We are unable to determine if this instability leads to a vortex glass state or simply represents a crossover to new critical exponents at the lower critical field.

I. INTRODUCTION

The equilibrium and dynamical properties of flux arrays in high-temperature (HTC) superconductors¹⁻⁷ have aroused considerable excitement and controversy during the past two years. Some aspects of the current debate are illustrated in Fig. 1, where we have for simplicity restricted our attention to magnetic fields aligned parallel to the c axis. In very clean samples, it is expected that

the conventional Abrikosov flux lattice will melt,^{3,4,8} leading to the schematic phase diagram shown in Fig. 1. A melted vortex liquid replaces the conventional Abrikosov flux lattice over a large region of the phase diagram because of the weak interplanar couplings, high temperatures, and short coherence lengths characteristic of the new HTC materials.³

Although extensive crystalline regions are clearly visible in flux-line decoration experiments at low fields and temperatures in some samples,⁹ there are undoubtedly circumstances in which disorder destroys the translational and orientational order of the Abrikosov flux lattice. Figure 1 shows an alternative phase diagram suggested by the authors of Ref. 5 for materials in which extrinsic impurity-induced disorder dominates at low temperatures. According to Ref. 5 the Abrikosov flux lattice may be replaced by a thermodynamically distinct vortex-glass phase, separated by a sharp transition line from a high-temperature vortex liquid. Even if there is no true vortex-glass phase, there will still be a gradual crossover from a low-temperature regime dominated by fluctuations in the impurity potential, to a high-temperature region dominated by thermal fluctuations. In this case, the dotted line in Fig. 1 would simply represent a locus of crossover temperatures.¹⁰

There is now evidence for a vortex-glass-phase transition, below which the linear resistivity vanishes, in epitaxially grown Y-Ba-Cu-O films.⁶ Although there are as yet few quantitative calculations, a phenomenological scaling theory provides a good fit to the measurements of Koch *et al.*⁶ The vortex-glass phenomenology does *not*, however, provide an adequate description of transport in much cleaner Y-Ba-Cu-O single-crystal samples studied recently by Worthington, Holtzberg, and Feild⁷ at least for the length scales probed by the most sensitive voltage-current measurements to date. The temperature at which the linear resistivity vanishes in these experiments was interpreted as the freezing of a flux liquid into an Abrikosov flux lattice (pinned by widely spaced strong pinning centers such as twin boundaries), consistent with a scenario first proposed by Gammel *et al.* on the basis of

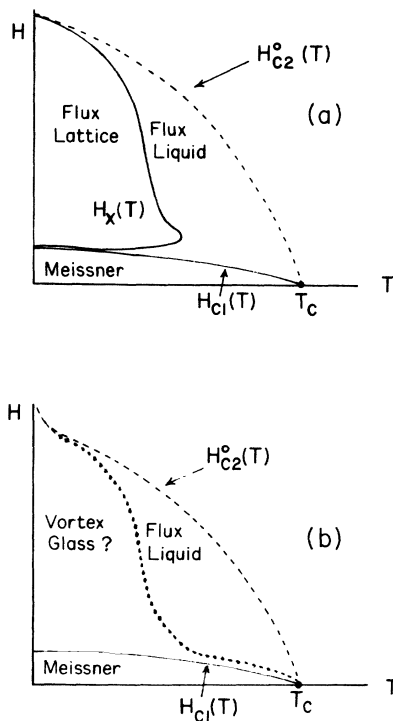


FIG. 1. (a) Phase diagram for pure HTC superconductors with magnetic field aligned with the c axis. (After Ref. 3.) (b) Phase diagram for HTC materials in the limit of strong disorder. (After Ref. 5.) The line $H_{c2}^0(T)$ marks the onset of the Meissner effect, and is not a true phase transition.

mechanical oscillator experiments.⁴ Even if pinning ultimately disrupts crystalline order on the longest length scales, the data of Worthington, Holtzberg, and Feild suggest that the relevant translational correlation lengths may be quite large.

It is natural to interpret the high-temperature regimes in all the above experiments in terms of a viscous flux liquid.¹¹ Although the intrinsic viscosity of decoupled planes of point vortices¹² is expected to be quite small, a large viscosity can arise from flux-line entanglement.³ Such a viscosity would be further augmented by the growing translational correlation length associated with a second-order (or nearly second-order) freezing transition. A large viscosity allows the effects of a few strong pinning centers (e.g., twin boundaries) to propagate over large distances in the flux liquid, and could also account qualitatively for the irreversible behavior observed by Malezoeff *et al.*² Obukhov and Rubinstein¹³ have recently suggested that enormous relaxation times (scaling with the exponential of the cube of the sample thickness) are possible in entangled flux liquids with large barriers to flux cutting. From this perspective, flux arrays below the “irreversibility line” would be in a nonequilibrium polymerlike glass state,³ dominated by the intrinsic disorder of entanglement as opposed to extrinsic impurity disorder.

The physical pictures sketched above represent a considerable departure from traditional ideas about flux lines in superconductors,¹⁴ and are far from universally accepted. One reason for the lack of consensus is the absence of direct information about actual flux-line configurations in HTC materials. Flux decoration experiments^{1,9} are very valuable, but are restricted to low fields and temperatures. Decorations, moreover, only show flux lines as they *emerge* from a HTC material and do not tell us how they meander (and possibly entangle) below the surface.¹⁵ It now appears that direct observations of flux arrays via neutron diffraction may be possible in HTC materials,¹⁶ just as in conventional superconductors.^{17,18} Neutron-diffraction probes three-dimensional flux-line configurations over a broad range of temperatures, including those at which flux-line motion precludes conventional decoration experiments.¹⁹

Neutron scattering provides information about the vortex line structure function,

$$S(q_1, q_z) = \langle |\hat{n}(q_1, q_z)|^2 \rangle, \quad (1.1)$$

where $\hat{n}(q_1, q_z)$ is the Fourier transform of the vortex line density

$$n(\mathbf{r}, z) = \sum_{j=1}^N \delta(\mathbf{r} - \mathbf{r}_j(z)). \quad (1.2)$$

The behavior of $S(q_1, q_z)$ for equilibrated flux liquids was worked out in Ref. 3 for very pure HTC materials, i.e., in the absence of disorder. The main point of this paper is to extend these calculations to the case of weak disorder.

There are two cases to consider. Sufficiently far from H_{c1} , correlations in melted flux liquids are only changed slightly by weak disorder: Disorder produces “Lorentzian-squared” corrections to the structure func-

tion found in Ref. 3. It would be particularly interesting to observe this effect by using neutron diffraction to monitor correlations in an initially clean crystal subjected to defect-producing radiation. Correlations in the tangent field,

$$\mathbf{t}(\mathbf{r}, z) = \sum_{j=1}^N \frac{d\mathbf{r}_j}{dz} \delta(\mathbf{r} - \mathbf{r}_j(z)), \quad (1.3)$$

which could, in principle, be probed via polarized neutron scattering, are also studied. Our results are obtained by mapping the statistical mechanics of vortex lines with impurities onto the physics of disordered bosons in two dimensions, as in the discussion of vortex glasses by M.P.A. Fisher.⁵ The simplified boson model we treat neglects nonlocal effects which are known to be quantitatively important at high fields in the crystalline phase.^{8,20} These arise because the magnetic field cannot follow fluctuations in the vortex cores at wavelengths shorter than the London penetration depth. The long-wavelength behavior of correlation functions with disorder can, however, be rederived by generalizing the simpler (and explicitly nonlocal) hydrodynamic approach of Ref. 11. Although the shear modulus of the Abrikosov flux lattice vanishes in a vortex liquid, the tilt and compressional moduli remain finite. Correlations in a dense vortex liquid with weak disorder can be described in terms of nonlocal tilt and compressional moduli which can be estimated from their crystalline phase values⁸ over a wide range of fields and temperatures.

Weak disorder produces only small corrections to the results for pure systems because its effects are “screened out” when the flux liquid is dense. The second case of interest occurs sufficiently close to H_{c1} , i.e., when the vortex lines are dilute and “screening” is no longer effective. In this limit, we find that disorder must produce new physics whenever

$$n_0 \lambda^2 \lesssim e^{-4\pi(k_B T)^3 / \bar{\epsilon}_1 \Delta}, \quad (1.4)$$

where n_0 is the average vortex areal density and λ is the (in-plane) London penetration depth. The quantity $\bar{\epsilon}_1$ is the tilt energy of a single vortex line and Δ is the variance of the random impurity potential [see Eq. (3.2) below]. Alternatively, we can say that disorder is certain to be *unimportant* provided

$$\xi_z \ll L_d, \quad (1.5)$$

where $\xi_z = 2\bar{\epsilon}_1 / k_B T n_0$ is the “entanglement correlation length” defined in Ref. 3, and L_d is a disorder-induced length scale in the z direction,

$$L_d = \frac{\bar{\epsilon}_1 \lambda^2}{k_B T} e^{4\pi(k_B T)^2 / \bar{\epsilon}_1 \Delta}. \quad (1.6)$$

When Eq. (1.5) is satisfied, a flux line suffers many collisions or entanglements with other vortices on scales less than L_d , thus “screening out” the effects of randomness.

The result (1.4) for the effect of disorder is not inconsistent with the phase diagram in Fig. 1, which shows a sliver of vortex-glass phase just above H_{c1} . We cannot exclude, however, the possibility that this instability sim-

ply represents a crossover to the new disorder-induced critical exponents at H_{c1} predicted by Natterman and Lipowsky.²¹ If there is, in fact, truly “glassy” behavior, it may be limited to the properties of a single vortex line precisely at H_{c1} .

The correlation functions calculated here pertain to the positions of the *vortex cores*. Information is provided about neutron scattering only to the extent that the magnetic field can follow the spatial fluctuations in the core positions. Vortex cores can twist and turn significantly on all spatial scales larger than the coherence length ξ . The magnetic field, however, can only follow the wanderings of the vortex core on scales larger than the London penetration depth $\lambda \gg \xi$. Direct applicability of our results to scattering experiments at wavelengths shorter than the London penetration depth would require a probe which scatters directly off the vortex cores. For pure systems, one can correct the correlation functions calculated here to make them directly relevant to magnetic-field fluctuations at essentially all wavelengths greater than the coherence length. We indicate how to do this in an appendix.

We have neglected here the potentially important issue of hexatic order in flux arrays.^{22–24} As pointed out by Chudnovsky,²³ the Larkin-Ovchinnikov model²⁵ of impurity disorder acting on an Abrikosov flux lattice leads to the destruction of translational order, but is insufficient to destroy long-range orientational order. The possibility of orientational correlation lengths which greatly exceed translational ones has not yet been considered by the vortex-glass phenomenologists.⁵ The recent observation of a low-temperature hexatic vortex glass in Ba-Sr-Ca-Cu-O (Ref. 24) suggests the possibility of an equilibrated hexatic vortex liquid at higher temperatures,²² and is consistent with a suggestion by Worthington, Holtzberg, and Feild⁷ for Y-Ba-Cu-O. The potential for hexatic order in flux liquids is important because a nonzero hexatic stiffness constant can increase the shear viscosity in vortex liquids.¹¹ The qualitative effect of hexatic order on the structure function of flux liquids (it leads to a sixfold in-plane anisotropy) has been discussed in Refs. 22 and 23. A detailed analysis of the effect of hexatic order on vortex line correlations is an interesting subject for future investigation.

In Sec. II we discuss correlations in pure flux liquids, and show that the results at long wavelengths also follow from a simple hydrodynamical approach. In Sec. III we introduce disorder into the hydrodynamical treatment and check the results against more microscopic calculations on a “disordered boson” model which neglects non-local effects. Finally, in Sec. IV, we show via renormalization-group methods that disorder does become relevant sufficiently close to H_{c1} and discuss the possibility of a vortex-glass phase in this limit. The relation of our results to magnetic correlation functions is sketched in Appendix A. In Appendix B, we show how the results for weak disorder can be recovered using the replica trick.

Some of the techniques used here (particularly the method for calculating tangent correlation functions) were developed in a study of oriented polymer liquid

crystals in a nematic solvent. Oriented polymers play the role of flux lines in this problem, with the important difference that the average polymer direction is a spontaneous, rather than externally imposed, broken symmetry. Details will appear in a future publication.²⁶

II. CORRELATIONS IN PURE FLUX LIQUIDS

A. Tangent and density correlations via the boson analogy

As shown in Fig. 2, we characterize vortex-line configurations by a set of N functions $\{\mathbf{r}_j(x)\}$ which specify the position of the j th vortex in the (x, y) plane as it wanders along the \hat{z} ($\hat{z} \parallel \mathbf{H}$) axis in a slab of thickness L .³ For now, we neglect the quenched random disorder shown in the figure. The probability of a particular configuration of N vortex lines is assumed to be proportional to $\exp(-\mathcal{S}_N/k_B T)$, where

$$\begin{aligned} \mathcal{S}_N = & \frac{1}{2} \bar{\epsilon}_1 \sum_{j=1}^N \int_0^L \left[\frac{d\mathbf{r}_j}{dz} \right]^2 dz \\ & + \frac{1}{2} \sum_{i \neq j} \int_0^L dz V(|\mathbf{r}_i(z) - \mathbf{r}_j(z)|) \\ & + \int dz \int d^2r \mathbf{h}(\mathbf{r}, z) \cdot \mathbf{t}(\mathbf{r}, z) . \end{aligned} \quad (2.1)$$

Here, $\bar{\epsilon}_1$ is the bending energy of the lines and $V(r)$ is an interaction potential, acting locally in each constant- z plane. We have assumed here that

$$\left| \frac{d\mathbf{r}_j}{dz} \right| \ll 1 .$$

Within the London theory, we have¹⁴

$$V(r) = \frac{\phi_0^2}{8\pi^2 \lambda^2} K_0(r/\lambda) , \quad (2.2)$$

where $\phi_0 = 2\pi\hbar c/2e$ is the flux quantum and $K_0(x)$ is a modified Bessel function. We found it useful to add a two-dimensional field $\mathbf{h}(\mathbf{r}, z)$ which couples to the local tangent field (1.3):

$$\int dz \int d\mathbf{r} \mathbf{h}(\mathbf{r}, z) \cdot \mathbf{t}(\mathbf{r}, z) = \sum_{j=1}^N \int_0^L dz \mathbf{h}(\mathbf{r}_j(z), z) \cdot \frac{d\mathbf{r}_j}{dz} . \quad (2.3)$$

If Z_N is the partition function obtained by integrating

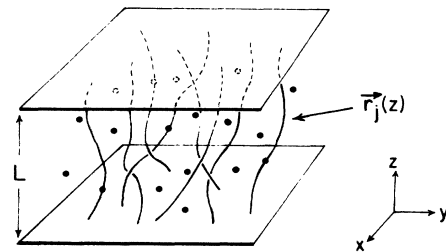


FIG. 2. Schematic of flux lines wandering through a sample in the presence of random impurities.

over all vortex line configurations,

$$Z_N = \frac{1}{N!} \prod_{j=1}^N \int \mathcal{D}\mathbf{r}_j(z) e^{-\delta_N/k_B T}, \quad (2.4)$$

the grand canonical partition sum is then

$$Z_{\text{gr}} = \sum_{N=0}^{\infty} e^{L\mu N/k_B T} Z_N, \quad (2.5)$$

where³ $\mu \propto H - H_{c1}$. The tangent-tangent correlation function is given by

$$\begin{aligned} \mathcal{T}_{ij}(\mathbf{r}, z) &= \langle t_i(\mathbf{r}, z) t_j(\mathbf{0}, 0) \rangle \\ &= (k_B T)^2 \frac{\delta^2}{\delta h_i(\mathbf{r}, z) \delta h_j(\mathbf{0}, 0)} \ln Z_{\text{gr}} \Big|_{\mathbf{h}=0}, \\ & \quad i, j = x, y. \end{aligned} \quad (2.6)$$

We shall also be interested in fluctuations in the vortex line density (1.2). If $n_0 = \langle n(\mathbf{r}, z) \rangle$ is the average vortex density, the vortex structure function is given by the Fourier transform of

$$S(\mathbf{r}, z) = \langle n(\mathbf{r}, z) n(\mathbf{0}, 0) \rangle \Big|_{\mathbf{h}=0} - n_0^2. \quad (2.7)$$

All averages are evaluated in the grand canonical ensemble.

At long wavelengths, the magnetic field can follow the fluctuations in the positions of the vortex cores, and the correlation functions (2.5) and (2.6) are directly related to fluctuations in the parallel and perpendicular magnetic field. A more general relation is constructed in Appendix A. Upon decomposing the local field $\mathbf{b}(\mathbf{r}, z)$ into fluctuations parallel and perpendicular to the average magnetic field direction $\mathbf{B}_0 \equiv \phi_0 n_0 \hat{z}$,

$$\mathbf{b}(\mathbf{r}, z) = \mathbf{B}_0 + \delta \mathbf{b}_{\parallel}(\mathbf{r}, z) + \delta \mathbf{b}_{\perp}(\mathbf{r}, z), \quad (2.8)$$

we find that the relations in Fourier space for *isotropic* superconductors are

$$\langle |\delta \mathbf{b}_{\parallel}(\mathbf{q}_1, q_z)|^2 \rangle = \frac{\phi_0^2}{(1 + \lambda^2 q^2)} S(\mathbf{q}_1, q_z) \quad (2.9)$$

and

$$\begin{aligned} \langle \delta b_{\perp, i}(\mathbf{q}_1, q_z) \delta b_{\perp, j}(-\mathbf{q}_1, -q_z) \rangle \\ = \frac{\phi_0^2}{(1 + \lambda^2 q^2)^2} T_{ij}(\mathbf{q}_1, q). \end{aligned} \quad (2.10)$$

We have neglected a small, additive, contribution which vanishes relative to the terms we have kept in the hydro-

dynamic limit. There are similar, but more complicated relations in the anisotropic case. See Appendix A.

As discussed in Ref. 3, there is a useful formal analogy between Eq. (2.4) and the imaginary time Feynman path integral for a set of fictitious quantum-mechanical particles in two dimensions interacting via an action given by Eq. (2.1). Temperature plays the role of Planck's constant. The calculations proceed in three steps: (1) The first quantized Lagrangian corresponding to Eq. (2.1) is transformed into the corresponding first quantized Hamiltonian. As shown in Ref. 3, only bosonic states contribute to the statistical mechanics associated with this Hamiltonian in the thermodynamic limit $L \rightarrow \infty$. (2) The Hamiltonian is rewritten in second quantized form. (3) The partition function for the second quantized Hamiltonian in the grand canonical ensemble is converted via a coherent state formalism²⁷ into an imaginary-time path integral. Calculations in this last representation can be done in a straightforward way,²⁸ provided one uses a renormalization procedure near H_{c1} .³

Because the auxiliary field $\mathbf{h}(\mathbf{r}, z)$ introduces extra velocity-dependent terms into the fictitious "Lagrangian," we must be careful in carrying out the first step described above. The real-time Lagrangian associated with Eq. (2.1) (with $z = it$) is

$$\mathcal{L} = \sum_{j=1}^N \left[\frac{1}{2} \tilde{\epsilon}_1 \left(\frac{d\mathbf{r}_j}{dt} \right)^2 + i \mathbf{h}_j \cdot \frac{d\mathbf{r}_j}{dt} \right] - \frac{1}{2} \sum_{i \neq j} V(|\mathbf{r}_i - \mathbf{r}_j|), \quad (2.11)$$

where $\mathbf{h}_j(z) = \mathbf{h}(\mathbf{r}_j(z), z)$. The "velocity" of the j th flux line is $\mathbf{q}_j = d\mathbf{r}_j/dt$, so the canonically conjugate momentum is

$$\mathbf{p}_j = \frac{\partial \mathcal{L}}{\partial \mathbf{q}_j} = \tilde{\epsilon}_1 \frac{d\mathbf{r}_j}{dt} + i \mathbf{h}_j. \quad (2.12)$$

The Hamiltonian is then

$$\begin{aligned} \mathcal{H} &= \sum_j \mathbf{p}_j \cdot \mathbf{q}_j - \mathcal{L} \\ &= \sum_j \left[\frac{\mathbf{p}_j^2}{2\tilde{\epsilon}_1} - \frac{i(\mathbf{h}_j \cdot \mathbf{p}_j + \mathbf{p}_j \cdot \mathbf{h}_j)}{2\tilde{\epsilon}_1} - \frac{\mathbf{h}_j^2}{2\tilde{\epsilon}_1} \right] \\ & \quad + \frac{1}{2} \sum_{i \neq j} V(|\mathbf{r}_i - \mathbf{r}_j|). \end{aligned} \quad (2.13)$$

The second quantized version of this Hamiltonian can be constructed using standard methods,^{27,29} with the result

$$\mathcal{H} = \int d^2 r \left[\frac{(k_B T)^2}{2\tilde{\epsilon}_1} |\nabla \hat{\psi}|^2 - \frac{k_B T}{2\tilde{\epsilon}_1} \mathbf{h} \cdot (\hat{\psi}^\dagger \nabla \psi - \hat{\psi} \nabla \psi^\dagger) - \frac{1}{2\tilde{\epsilon}_1} h^2 |\hat{\psi}|^2 \right] + \frac{1}{2} \int d^2 r \int d^2 r' \hat{\psi}^\dagger(\mathbf{r}) \hat{\psi}^\dagger(\mathbf{r}') V(\mathbf{r} - \mathbf{r}') \hat{\psi}(\mathbf{r}') \hat{\psi}(\mathbf{r}), \quad (2.14)$$

where $\hat{\psi}^\dagger(\mathbf{r})$ and $\psi(\mathbf{r})$ are boson creation and destruction operators. A coherent state path-integral representation of the grand canonical partition sum associated with (2.14) leads to

$$Z_{\text{gr}} = \int \mathcal{D}\psi(\mathbf{r}, z) \int \mathcal{D}\psi^*(\mathbf{r}, z) e^{-\delta[\psi, \psi^*]/k_B T}, \quad (2.15)$$

where $\psi(\mathbf{r}, z)$ is a complex field and the ‘‘action’’ in the imaginary-time path integral (2.14) is

$$\mathcal{S}[\psi, \psi^*] = \int d^2r \int dz \left[\psi^* \left[k_B T \frac{\partial}{\partial z} - \frac{(k_B T)^2}{2\bar{\epsilon}_1} \nabla^2 - \mu \right] \psi - \frac{(k_B T)^2}{2\bar{\epsilon}_1} \mathbf{h} \cdot (\psi^* \nabla \psi - \psi \nabla \psi^*) - \frac{1}{2\bar{\epsilon}_1} h^2 |\hat{\psi}|^2 \right] + \frac{1}{2} V_0 |\psi|^4. \quad (2.16)$$

We have, for simplicity, now approximated the potential (2.2) by

$$V(\mathbf{r}) \approx V_0 \delta(\mathbf{r}), \quad (2.17)$$

where

$$V_0 = \int d^2r V(r) = \phi_0^2 / 4\pi. \quad (2.18)$$

It is, however, easy to repeat the calculations for an arbitrary pair potential (see below).

Following Refs. 3 and 28, we assume $H \gg H_{c1}$ (i.e., the flux lines are dense) and expand about the minimum of (2.15) in mean-field theory. Accordingly, we set

$$\psi(\mathbf{r}, z) = \sqrt{n_0 + \pi(\mathbf{r}, z)} e^{i\theta(\mathbf{r}, z)} \approx \sqrt{n_0} \left[1 + \frac{1}{2n_0} \pi(\mathbf{r}, z) + \dots \right] e^{i\theta(\mathbf{r}, z)}, \quad (2.19)$$

where $n_0 = \mu / V_0$. Upon expanding Eq. (2.15) in the field $\pi(\mathbf{r}, z)$, and neglecting an overall constant as well as surface terms, we find the quadratic (in θ , π , and \mathbf{h}) effective action

$$\mathcal{S}_{\text{eff}} = \int d^2r \int dz \left[\frac{1}{2} V_0 \pi^2 + \frac{(k_B T)^2}{8n_0 \bar{\epsilon}_1} |\nabla \pi|^2 + \frac{(k_B T)^2 n_0}{2\bar{\epsilon}_1} |\nabla \theta|^2 - \frac{(k_B T)^2}{\bar{\epsilon}_1} (in_0 \mathbf{h} \cdot \nabla \theta + \frac{1}{2} n_0 h^2) + i\pi \frac{\partial \theta}{\partial z} \right]. \quad (2.20)$$

Upon defining Fourier transformed variables

$$\theta(\mathbf{r}, z) = \int \frac{d^2q_{\perp}}{(2\pi)^2} \int \frac{dq_z}{2\pi} e^{i\mathbf{q}_{\perp} \cdot \mathbf{r} + iq_z z} \theta(\mathbf{q}_{\perp}, q_z) \quad (2.21)$$

and

$$\pi(\mathbf{r}, z) = \int \frac{d^2q_{\perp}}{(2\pi)^2} \int \frac{dq_z}{2\pi} e^{i\mathbf{q}_{\perp} \cdot \mathbf{r} + iq_z z} \pi(\mathbf{q}_{\perp}, q_z), \quad (2.22)$$

and similarly for $h(\mathbf{r}, z)$, the effective action takes the form

$$\mathcal{S}_{\text{eff}} = \int \frac{d^3q}{(2\pi)^3} \left[\frac{1}{2} X^{\dagger}(\mathbf{q}) G^{-1}(\mathbf{q}) X(\mathbf{q}) - \frac{n_0 k_B T}{2\bar{\epsilon}_1} \mathbf{q}_{\perp} \cdot [\mathbf{h}(\mathbf{q}) \theta^*(\mathbf{q}) - \mathbf{h}^*(\mathbf{q}) \theta(\mathbf{q})] + \frac{n_0}{2\bar{\epsilon}_1} |\mathbf{h}(\mathbf{q})|^2 \right], \quad (2.23)$$

where $\mathbf{q} = (\mathbf{q}_{\perp}, q_z)$, $X(\mathbf{q})$ is the column vector

$$X(\mathbf{q}) = \begin{pmatrix} \theta(\mathbf{q}) \\ \pi(\mathbf{q}) \end{pmatrix} \quad (2.24)$$

and the coefficient matrix is

$$G^{-1}(\mathbf{q}) = \begin{pmatrix} \frac{n_0 (k_B T)^2 q_{\perp}^2}{\bar{\epsilon}_1} & -q_z k_B T \\ q_z k_B T & V_0 + \frac{(k_B T)^2 q_{\perp}^2}{8n_0 \bar{\epsilon}_1} \end{pmatrix}. \quad (2.25)$$

We can now calculate the tangent correlation function T_{ij} within this quadratic expansion about mean-field theory by using the thermodynamic formula (2.6) and assuming that fluctuations occur with a probability proportional to $\exp(-\mathcal{S}_{\text{eff}}/k_B T)$. The result is

$$T_{ij}(\mathbf{q}_\perp, q_z) = \int d^2r \int dz e^{-i\mathbf{q}_\perp \cdot \mathbf{r} - iq_z z} T_{ij}(\mathbf{r}, z) = \frac{k_B T n_0}{\bar{\epsilon}_1} \left[\delta_{ij} - \frac{q_{i\perp} q_{j\perp}}{q_\perp^2} \right] + \frac{k_B T n_0}{\bar{\epsilon}_1} \frac{q_z^2}{q_z^2 + \epsilon^2(q_\perp)} / (k_B T)^2 \frac{q_{i\perp} q_{j\perp}}{q_\perp^2} \\ \equiv A(\mathbf{q}_\perp, q_z) P_{ij}^T(\mathbf{q}_\perp) + B(\mathbf{q}_\perp, q_z) P_{ij}^L(\mathbf{q}_\perp), \quad (2.26)$$

where $\epsilon(q_\perp)$ is the well-known Bogoliubov excitation spectrum of a weakly interacting superfluid,

$$\frac{\epsilon(q_\perp)}{k_B T} = \left[\left(\frac{k_B T q_\perp^2}{2\bar{\epsilon}_1} \right)^2 + \frac{n_0 V_0}{\bar{\epsilon}_1} q_\perp^2 \right]^{1/2} \quad (2.27)$$

and $P_{ij}^T(\mathbf{q}_\perp)$ and $P_{ij}^L(\mathbf{q}_\perp)$ are two-dimensional transverse and longitudinal projection operators. The density-density correlation function is³

$$S(\mathbf{q}_\perp, q_z) = \int d^2r \int dz e^{-i\mathbf{q}_\perp \cdot \mathbf{r} - iq_z z} S(\mathbf{r}, t) \\ = \frac{k_B T n_0}{\bar{\epsilon}_1} \frac{q_\perp^2}{q_z^2 + \epsilon^2(q_\perp)} / (k_B T)^2. \quad (2.28)$$

To generalize these results to an arbitrary pair potential $V(\mathbf{r})$, let $V_0 \rightarrow \hat{V}(\mathbf{q})$ in Eq. (2.27), where $\hat{V}(\mathbf{q})$ is the Fourier transform of $V(\mathbf{r})$. It can be shown that $A(0, q_z) = B(0, q_z) = k_B T n_0 / \bar{\epsilon}_1$ is an exact property of the model (2.1), using the transformation properties of the Lagrangian under a ‘‘Galilean transformation,’’

$$\frac{d\mathbf{r}_j}{dz} \rightarrow \frac{d\mathbf{r}_j}{dz} + \mathbf{h} / \bar{\epsilon}_1.$$

These correlation functions describe the wandering of flux lines in an equilibrated flux liquid in the absence of disorder. A crucial constraint on the statistical mechanics arises because flux lines can neither stop nor start inside the medium,

$$\partial_z n + \nabla \cdot \mathbf{t} = 0. \quad (2.29)$$

This constraint is automatically satisfied by the path-integral formalism embodied in Eqs. (2.14) and (2.15), because of the invariance of the action (2.15) under $\psi \rightarrow \psi e^{i\theta_0}$. The constraint (2.29) implies in particular that density fluctuations are related to the longitudinal part of the tangent field,

$$S(\mathbf{q}_\perp, q_z) = (q_\perp^2 / q_z^2) B(\mathbf{q}_\perp, q_z), \quad (2.30)$$

a condition which is satisfied by Eqs. (2.26) and (2.28). We can also use Eq. (2.29) to relate mixed correlation functions like $\langle \pi(\mathbf{q}) t_j(-\mathbf{q}) \rangle$ to $B(\mathbf{q})$. We have

$$\langle \pi(\mathbf{q}) t_j(-\mathbf{q}) \rangle = (-q_{\perp,i} / q_z) T_{ij}(\mathbf{q}) \\ = -(q_{\perp,j} / q_z) B(\mathbf{q}_\perp, q_z),$$

implying that $\delta \mathbf{b}_\parallel$ and $\delta \mathbf{b}_\perp$ in Eq. (2.8) are correlated. When reexpressed in terms of the magnetic field in the long-wavelength limit, Eq. (2.29) is just the constraint of no magnetic monopoles, $\nabla \cdot \mathbf{b} = 0$.

The vortex-line correlation function (2.28) is missing the δ function Bragg peaks surrounded by thermal diffuse scattering at reciprocal lattice positions expected for the Abrikosov flux lattice.³ The *long-wavelength* behavior, however, is simply related to that expected near the origin for a thermally excited flux crystal. To see this, we

first rewrite (2.26) and (2.28) in the limit of small q_\perp and q_z ,

$$T_{ij}(q_\perp, q_z) \approx \frac{n_0^2 k_B T}{n_0 \bar{\epsilon}_1} P_{ij}^T(\mathbf{q}_\perp) \\ + \frac{n_0^2 k_B T q_z^2}{n_0 \bar{\epsilon}_1 q_z^2 + V_0 n_0^2 q_\perp^2} P_{ij}^L(\mathbf{q}_\perp), \quad (2.31)$$

$$S(\mathbf{q}_\perp, q_z) \approx \frac{n_0^2 k_B T q_\perp^2}{n_0 \bar{\epsilon}_1 q_z^2 + V_0 n_0^2 q_\perp^2}. \quad (2.32)$$

Fluctuations in the crystalline phase, on the other hand, are controlled by a continuum elastic free energy,³⁰

$$F = \frac{1}{2} \int \frac{d^2 q_\perp}{(2\pi)^2} \int \frac{dq_z}{2\pi} \{ (K q_z^2 + \mu q_\perp^2) P_{ij}^T(\mathbf{q}_\perp) \\ + [K q_z^2 + (B + \mu) q_\perp^2] P_{ij}^L(\mathbf{q}_\perp) \} \\ \times u_i(\mathbf{q}) u_j(-\mathbf{q}), \quad (2.33)$$

where μ , K , and B are, respectively, the shear, tilt, and bulk modulus and $\mathbf{u}(\mathbf{q})$ is the Fourier transformed vortex displacement field. We have, for simplicity, neglected the nonlocal character of the elastic constants.^{8,20} It is easy to show that the variables $\pi(\mathbf{r}, z)$ and $\mathbf{t}(\mathbf{r}, z)$ are related in the solid phase to the displacement field,

$$\pi(\mathbf{r}, z) = -n_0 \nabla_\perp \cdot \mathbf{u}(\mathbf{r}, z), \quad (2.34)$$

$$\mathbf{t}(\mathbf{r}, z) = n_0 \frac{\partial \mathbf{u}(\mathbf{r}, z)}{\partial z}.$$

Fluctuations in the crystal occur with probability proportional to $\exp(-F/k_B T)$, and it then follows from Eq. (2.33) that

$$T_{ij}(q_\perp, q_z) = \frac{n_0^2 k_B T q_z^2}{K q_z^2 + \mu q_\perp^2} P_{ij}^T(\mathbf{q}_\perp) \\ + \frac{n_0^2 k_B T q_z^2}{K q_z^2 + (B + \mu) q_\perp^2} P_{ij}^L(\mathbf{q}_\perp), \quad (2.35)$$

$$S(q_\perp, q_z) = \frac{n_0^2 k_B T q_\perp^2}{K q_z^2 + (B + \mu) q_\perp^2}. \quad (2.36)$$

We see that the solid phase results agree with those in the liquid provided we set the shear modulus $\mu = 0$ and make the identifications

$$K = n_0 \bar{\epsilon}_1 \quad (2.37)$$

and

$$B = n_0^2 V_0. \quad (2.38)$$

These are precisely the tilt and bulk moduli one expects for the simple model of interacting flux lines summarized

in Eq. (2.1).³ Note that although the long-wavelength behaviors of the longitudinal part of $T_{ij}(\mathbf{q}_1, q_z)$ and of $S(\mathbf{q}_1, q_z)$ are qualitatively similar in the liquid and solid phases, the *transverse* part of $T_{ij}(\mathbf{q}_1, q_z)$ behaves very differently in these two cases.

We conclude this section with a discussion of the validity of the fluctuation-corrected mean-field approximation used here. The critical point of the field theory described by (2.16) occurs for $\mu \approx 0$, i.e., for $H \approx H_{c1}$. To avoid having to deal with critical fluctuations, we have assumed that the flux lines are dense so that $\mu \gg 0$. Of course, if the flux lines are dense, higher-order terms in the “order parameter” ψ representing higher-order interactions between vortex lines will become important in Eq. (2.16). One can still, however, make the expansion (2.19) about the minimum of the potential, although the mean flux density will no longer be given by $n_0 = \mu/V_0$. We expect that the hydrodynamic form of the results presented here will be unchanged, except for modifications, e.g., in the parameter V_0 appearing in Eq. (2.27).

With appropriate modifications, the Bogoliubov results are expected to become *quantitatively* accurate in the *dilute* limit. In a *three-dimensional* superfluid gas, one sums an infinite series of diagrams and sees that the bare potential in Hamiltonians such as Eq. (2.14) should be replaced by an effective “*t* matrix” which is proportional to the *s*-wave scattering amplitude.³¹ This procedure means that the Bogoliubov results give the leading order terms in an expansion in powers of $(n_0\lambda^3)^{1/2}$, where n_0 is the boson density and λ is the range of the interaction. In the two-dimensional case of interest here, an analogous diagrammatic summation³² leads in the dilute limit to the replacement

$$\frac{V_0 \bar{\epsilon}_1}{(k_B T)^2} \rightarrow \frac{V_0 \bar{\epsilon}_1 / (k_B T)^2}{1 + [V_0 \bar{\epsilon}_1 / (k_B T)^2] \ln(1/n\lambda^2) / 4\pi} \approx \frac{4\pi}{\ln(1/n\lambda^2)}, \quad (2.39)$$

and an expansion in $1/\ln(1/n\lambda^2)$. Upon defining the dimensionless wave vectors

$$\mathbf{k}_1 = \mathbf{q}_1 \xi_1, \quad k_z = q_z \xi_z, \quad (2.40)$$

where $\xi_1 = n^{-1/2}$ is the intervortex spacing and

$$\xi_z = \frac{2\bar{\epsilon}_1}{nk_B T}$$

is the “entanglement correlation length,” the structure function with this replacement becomes³

$$S(\mathbf{q}_1, q_z) = n_0^2 \frac{\xi_z^2}{51 \xi_z} \frac{2k_1^2}{k_z^2 + k_1^4 + \frac{\pi}{\ln(1/n\lambda^2)} k_1^2}. \quad (2.41)$$

Note that the very large bare value of the dimensionless interaction strength

$$v = V_0 \bar{\epsilon}_1 / (k_B T)^2, \quad (2.42)$$

which is of order 10^5 even in HTC materials,³ has

dropped out.

The contours of constant scattering for Eq. (2.36) are shown in Fig. 3 for $n\lambda^2 = 0.1$. In a dense, as opposed to dilute, flux liquid we would expect a peak along the $q_z = 0$ axis when $q_1 \approx 2\pi/d$. A δ function Bragg peak would appear at roughly this position in the crystalline phase. As discussed in Ref. 3, the finite Lorentzian width of the structure function in the q_z direction when $q_1 \sim 1/d$ (as opposed to the infinitely sharp Bragg peak in the solid) measures the degree of entanglement of the flux lines along the z axis.

Although the Bogoliubov spectrum (2.23) is not expected to be quantitatively accurate for dense superfluids, and, hence, for dense configurations of flux lines, we can improve the theory by following Feynman and approximating this spectrum by³³

$$\epsilon(q_1) = \frac{(k_B T)^2 q_1^2}{2\bar{\epsilon}_1 S_2(q_1)}, \quad (2.43)$$

where $S_2(q_1)$ is the structure function of the dense vortex liquid in a constant- z cross section.³ When typical two-dimensional liquid structure functions are used, this approximation leads to a “roton” minimum in the excitation spectrum and to a peak in³⁴

$$S(\mathbf{q}_1, q_z) = \frac{n_0 k_B T q_1^2 / \bar{\epsilon}_1}{q_z^2 + \left[\frac{k_B T q_1^2}{2\bar{\epsilon}_1 S_2(q_1)} \right]^2} \quad (2.44)$$

along the q_1 axis at $q_1 \approx 2\pi n^{1/2}$.

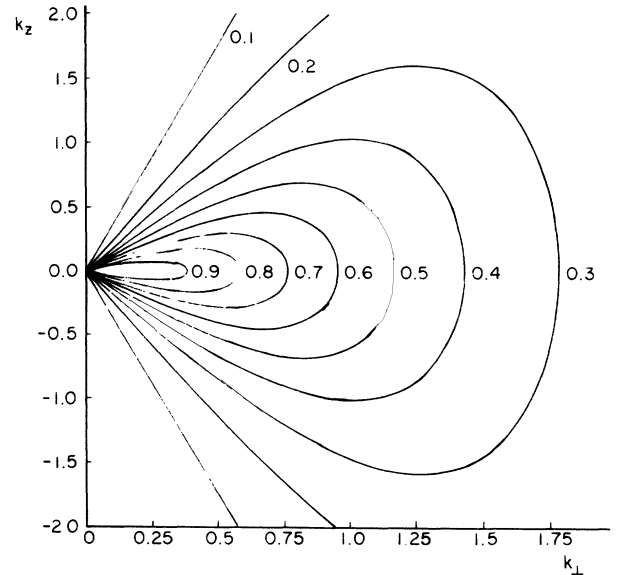


FIG. 3. Constant intensity contours of the structure function (2.33) in the Bogoliubov approximation appropriate to the dilute limit. The structure function is normalized so that it approaches unity when the origin is approached along the line $k_z = 0$. Dense vortex liquids should display a Lorentzian peak along this axis at $k_1 \approx 2\pi$, corresponding to the smallest reciprocal lattice vector of a flux crystal at the same density.

B. Correlations from hydrodynamics

Although the simple model interacting flux lines discussed above gives insights into the qualitative behavior of entangled flux liquids, it neglects nonlocal effects which are known to be quantitatively important in flux crystals over much of the temperature-field phase diagram.^{8,20} We show here how the long-wavelength behavior of the correlations discussed above can be easily extracted from a hydrodynamic description of flux liquids which takes these nonlocal effects into account.¹¹ By long wavelengths, we mean wavelengths large compared to the spacing between CuO_2 planes in the \hat{z} direction,

and wavelengths long compared to the spacing between flux lines perpendicular to \hat{z} . A related hydrodynamic approach to correlations in polymer nematic liquid crystals was proposed long ago by de Gennes³⁵ and has been developed more recently by Selinger and Bruinsma.³⁶ The boson mapping is applied to this system in Ref. 26.

Following Ref. 11, we expand the free energy of the flux liquid in the deviation

$$\delta n(\mathbf{r}, z) = n(\mathbf{r}, z) - n_0 \equiv \pi(\mathbf{r}, z)$$

of the line density (1.2) from its average value n_0 and in the tangent density (1.3),

$$F_L = \frac{1}{2n_0^2} \int d^2r dz \int d^2r' dz' [K(|\mathbf{r}-\mathbf{r}'|, z-z') \mathbf{t}(\mathbf{r}, z) \cdot \mathbf{t}(\mathbf{r}', z') + B(|\mathbf{r}-\mathbf{r}'|, z-z') \delta n(\mathbf{r}, z) \delta n(\mathbf{r}', z')] . \quad (2.45)$$

The functions $K(r, z)$ and $B(r, z)$ are liquid-phase generalizations of the nonlocal tilt and bulk moduli of Refs. 8 and 20. The shear modulus of the flux liquid is zero. (For an explicit demonstration that the shear modulus vanishes in a *hexatic* vortex liquid, see Ref. 22.) It is possible to write a model of interacting flux lines in isotropic superconductors proposed by Brandt³⁷ in precisely this form, and read off the functions $K(r, z)$ and $B(r, z)$. Although $K(r, z)$ and $B(r, z)$ are harder to calculate for an anisotropic HTC superconductor, their values for flux liquids in high fields are probably quite similar to those in the crystalline phase,⁸ where K and B are typically much larger than the shear modulus. In the hydrodynamic limit, it is appropriate to integrate over the smoothly varying hydrodynamic fields $\mathbf{t}(\mathbf{r}, z)$ and $\delta n(\mathbf{r}, z)$, even though the underlying degrees of freedom in the definitions (1.2) and (1.3) are discrete flux lines. The approximation involved is similar to the "Debye-Hückel approximation" often applied to a discrete point vortex "plasma" in two dimensions above the Kosterlitz-Thouless transition.³⁸

The probability of a fluctuation is proportional to $\exp(-F_L/k_B T)$, but averages must of course be carried out subject to the constraint (2.29). We shall implement this constraint in Fourier space, so that the thermal average of a quantity Q is defined by

$$\langle Q \rangle = \frac{\int \mathcal{D}\mathbf{t}(\mathbf{q}) \int \mathcal{D}\delta n(\mathbf{q}) \left[\prod_{\mathbf{p}} \delta(p_z \delta n(\mathbf{p}) + \mathbf{p}_1 \cdot \mathbf{t}(\mathbf{p})) \right] Q \exp(-F_L/k_B T)}{\int \mathcal{D}\mathbf{t}(\mathbf{q}) \int \mathcal{D}\delta n(\mathbf{q}) \left[\prod_{\mathbf{p}} \delta(p_z \delta n(\mathbf{p}) + \mathbf{p}_1 \cdot \mathbf{t}(\mathbf{p})) \right] \exp(-F_L/k_B T)} . \quad (2.46)$$

With this definition, it is easy to show that

$$T_{ij}(\mathbf{q}_L, q_z) = \frac{n_0^2 k_B T}{\hat{K}(\mathbf{q})} P_{ij}^T(\mathbf{q}_L) + \frac{n_0^2 k_B T q_z^2}{\hat{K}(\mathbf{q}) q_z^2 + \hat{B}(\mathbf{q}) q_1^2} P_{ij}^L(\mathbf{q}_L) \quad (2.47)$$

and

$$S(\mathbf{q}_L, q_z) = \frac{n_0^2 k_B T q_1^2}{\hat{K}(\mathbf{q}) q_z^2 + \hat{B}(\mathbf{q}) q_1^2} , \quad (2.48)$$

where $\hat{K}(\mathbf{q})$ and $\hat{B}(\mathbf{q})$ are the Fourier transforms of $K(r, z)$ and $B(r, z)$. We see that these correlations are identical in form to Eqs. (2.31) and (2.32), except that the elastic constants (2.37) and (2.38) are replaced by wavevector-dependent quantities. Using the *crystal*-phase values of Houghton, Pelcovits, and Sudbo⁸ to approximate $K(q_1, q_z)$ and $B(q_1, q_z)$ we have plotted the contours of $S(q_1, q_z)$ in Fig. 4. We have plotted the dimensionless *reduced* structure function

$$\bar{S}(q_1, q_z) \equiv \frac{H^2(1-h)}{8\pi h \kappa^2} \frac{q_1^2}{\hat{K}(q_1, q_z) q_z^2 + \hat{B}(q_1, q_z) q_1^2} , \quad (2.49)$$

where $h = H/H_{c2}$, $\kappa = \lambda/\xi$, and $\hat{K}(\mathbf{q}) = c_{44}(\mathbf{q})$, $\hat{B}(\mathbf{q}) = c_{11}(\mathbf{q})$ in the notation of Houghton, Pelcovits, and Sudbo.⁸ The parameters are those for Y-Ba-Cu-O at $T = 77$ K and $H = 0.5$ T. The change in slope in these contours reflects the strong dependence of the elastic constants on wave vector. There is a small critical value of

$$\bar{S} = \bar{S}^* = \frac{H^2(1-h)}{8\pi h \kappa^2} \frac{1}{B(0,0)} \approx 0.02$$

below which the contours all come in linearly at the origin, as in Fig. 3. These contours are not shown in the figure.

III. WEAK DISORDER

A. Hydrodynamic treatment

We first extend the simplified hydrodynamic discussion of Sec. II B to the case of weak disorder. Our conclusions

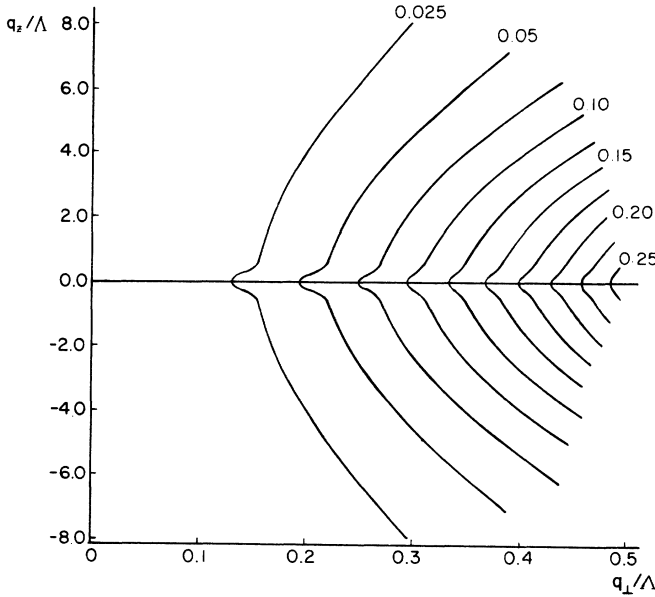


FIG. 4. Constant intensity contours of the reduced structure function (2.49) as a function of q_{\perp}/Λ and q_z/Λ , where $\Lambda = \sqrt{2H/H_{c25}}$ is the radius of the circular Brillouin zone discussed in Ref. 8, as obtained from the hydrodynamic theory discussed in the text.

will then be checked via an explicit calculation using the model of disordered bosons considered by M.P.A. Fisher.⁵ To model disorder microscopically, we must add to Eq. (2.1) a term

$$F_L = \frac{1}{2n_0^2} \int d^2r dz \int d^2r' dz' [K(|\mathbf{r}-\mathbf{r}'|, z-z') \mathbf{t}(\mathbf{r}, z) \cdot \mathbf{t}(\mathbf{r}', z') + B(\mathbf{r}-\mathbf{r}', z-z') \delta n(\mathbf{r}, z) \delta n(\mathbf{r}', z')] + \int d^2r dz V_D(\mathbf{r}, z) \delta n(\mathbf{r}, z). \quad (3.5)$$

Upon passing to Fourier space and making a \mathbf{q} -dependent shift in $\delta n(\mathbf{q}_{\perp}, q_z)$, the annealed averages over $\mathbf{t}(\mathbf{r}, z)$ and $\delta n(\mathbf{r}, z)$ can be carried out as in Sec. II B. After carrying out both the thermal average and an average over the quenched random disorder, we readily find

$$\overline{T_{ij}(\mathbf{q}_{\perp}, q_z)} \equiv \overline{\langle t_i(\mathbf{q}) t_j(-\mathbf{q}) \rangle} = k_B T \frac{n_0^2}{\hat{K}(\mathbf{q}_{\perp}, q_z)} P_{ij}^T(q_{\perp}) + \left[k_B T \frac{n_0^2 q_z^2}{\hat{K}(\mathbf{q}) q_z^2 + \hat{B}(\mathbf{q}) q_{\perp}^2} + \Delta \left(\frac{n_0^2 q_{\perp} q_z}{\hat{K}(\mathbf{q}) q_z^2 + \hat{B}(\mathbf{q}) q_{\perp}^2} \right)^2 \right] P_{ij}^L(\mathbf{q}_{\perp}), \quad (3.6)$$

$$\overline{S(\mathbf{q}_{\perp}, q_z)} \equiv \overline{\langle |\delta n(\mathbf{q})|^2 \rangle} = k_B T \frac{n_0^2 q_{\perp}^2}{\hat{K}(\mathbf{q}) q_z^2 + \hat{B}(\mathbf{q}) q_{\perp}^2} + \Delta \left(\frac{n_0^2 q_{\perp}^2}{\hat{K}(\mathbf{q}) q_z^2 + \hat{B}(\mathbf{q}) q_{\perp}^2} \right)^2. \quad (3.7)$$

Disorder introduces a ‘‘Lorentzian-squared’’ correction to the hydrodynamic result (2.48) for the density correlation function, with a similar correction for the longitudinal part of the tangent correlation function (2.47). The transverse part of the tangent correlations is unrenormalized. The calculations are equally straightforward if we introduce a quenched random field which couples linearly to the tangent vector.

B. Calculations within the boson model

The boson mapping can be used to calculate correlations directly from a more microscopic action with disorder, namely,

$$\delta \mathcal{S} = \sum_{j=1}^N \int dz V_D(\mathbf{r}_j(z), z), \quad (3.1)$$

where the random potential $V_D(\mathbf{r}, z)$ represents the effects of impurities. If the defects are randomly distributed, as in the case of, say, oxygen vacancies,³⁹ we expect that quenched fluctuations in the impurity potential will obey

$$\overline{V_D(\mathbf{r}, z) V_D(\mathbf{r}', z')} = \Delta \delta(\mathbf{r}-\mathbf{r}') \delta(z-z'), \quad (3.2)$$

with $\overline{V_D(\mathbf{r}, z)} = 0$. The overbar represents an average over the impurity disorder. An explicit formula for the coefficient Δ is given by Fisher, Fisher, and Huse,⁵ namely,

$$\Delta \approx \frac{1}{4} \gamma_I^2 v_c n_I [T_c / (T_c - T)]^2 (\phi_0^4 / 16\pi^2 \lambda^2), \quad (3.3)$$

where v_c is the volume of the unit cell in the underlying crystal, n_I is the fraction of impurities in this cell, and

$$\gamma_I = d[\ln T_C(n_I)] / dn_I$$

is a dimensionless impurity coupling constant (typically of order unity).

Note first that we can rewrite Eq. (3.1) as

$$\delta \mathcal{S} = \int d^2r \int dz V_D(\mathbf{r}, z) \delta n(\mathbf{r}, z), \quad (3.4)$$

where $\delta n(\mathbf{r}, z) = n(\mathbf{r}, z) - n_0$ and we have used Eq. (1.2) and the fact that the spatial average of the impurity potential vanishes. This suggests that we model disorder by adding an extra term to Eq. (2.45),

$$\mathcal{S}_N = \frac{1}{2}\bar{\epsilon}_1 \sum_{j=1}^N \int_0^L \left[\frac{d\mathbf{r}_j}{dz} \right]^2 dz + \frac{1}{2} \sum_{i \neq j} \int_0^L dz V(|\mathbf{r}_i - \mathbf{r}_j|) + \sum_{j=1}^N \int_0^L dz V_D(\mathbf{r}_j(z), z). \quad (3.8)$$

Upon carrying out the transformations discussed in Sec. II A, we find that we must evaluate a partition function like Eq. (2.15), but with Eq. (2.16) replaced by

$$\mathcal{S}[\psi, \psi^*] = \int d^2r \int dz \left[\psi^* \left[k_B T \frac{\partial}{\partial z} - \frac{(k_B T)^2}{2\bar{\epsilon}_1} \nabla^2 - \mu - \delta\mu(\mathbf{r}, z) \right] \psi + \frac{1}{2} V_0 |\psi|^4 \right]. \quad (3.9)$$

We must of course average the *logarithm* of the partition function over the quenched random chemical potential $\delta\mu(\mathbf{r}, z) = V_D(\mathbf{r}, z)$, with a related quenched averaging procedure for correlations. This is the model considered in Ref. 5 as the basis of the phenomenological vortex-glass proposal. Here, we repeat the fluctuation-corrected mean-field treatment of Sec. II A in the limit of weak disorder, and show explicitly that disorder merely introduces ‘‘Lorentzian-squared’’ corrections in the vortex liquid like those found in the hydrodynamic limit above. The limit of strong disorder, which becomes relevant near H_{c1} , will be treated in Sec. IV. We discuss explicitly only density correlations; the calculations for tangent correlations are very similar.

Upon making the decomposition (2.19), and keeping only quadratic terms in $\pi(\mathbf{r}, z)$ and $\theta(\mathbf{r}, z)$, we find that the effective action (2.17) is replaced by

$$\mathcal{S}_{\text{eff}} = \int d^2r \int dz \left[\frac{1}{2} V_0 \pi^2 + \frac{(k_B T)^2}{8n_0 \bar{\epsilon}_1} |\nabla \pi|^2 + \frac{k_B T n_0}{2\bar{\epsilon}_1} |\nabla \theta|^2 + i\pi \frac{\partial \theta}{\partial z} - \delta\mu \pi \right], \quad (3.10)$$

which becomes

$$\mathcal{S}_{\text{eff}} = \int \frac{d^3q}{(2\pi)^2} \left[\frac{1}{2} X^\dagger(\mathbf{q}) G^{-1}(\mathbf{q}) X(\mathbf{q}) - \delta\mu(\mathbf{q}) \pi(-\mathbf{q}) \right] \quad (3.11)$$

with the definitions (2.24) and (2.25). It is now easy to evaluate the necessary annealed and quenched averages and find

$$\overline{S(\mathbf{q}_\perp, q_z)} = k_B T \frac{(n_0 q_\perp^2 / \bar{\epsilon}_1)}{q_z^2 + \varepsilon^2(q_\perp) / (k_B T)^2} + \Delta \left[\frac{(n_0 q_\perp^2 / \bar{\epsilon}_1)}{q_z^2 + \varepsilon^2(q_\perp) / (k_B T)^2} \right]^2, \quad (3.12)$$

where $\varepsilon(q_\perp)$ is the Bogoliubov spectrum (2.27). Disorder produces a ‘‘Lorentzian-squared’’ correction, just as in our hydrodynamic treatment. For small Δ , the fluctuation-corrected mean-field theory used here should be adequate provided we are far from H_{c1} . It is tedious, but straightforward to derive the tangent-tangent correlation function by the method of Sec. II A. The result is

$$\overline{T_{ij}(\mathbf{q}_\perp, q_z)} = \frac{k_B T n_0}{\bar{\epsilon}_1} P_{ij}^T(\mathbf{q}_\perp) + \left[k_B T \frac{(n_0 q_z^2 / \bar{\epsilon}_1)}{q_z^2 + \varepsilon^2(q_\perp) / (k_B T)^2} + \Delta \left[\frac{(n_0 q_\perp q_z / \bar{\epsilon}_1)}{q_z^2 + \varepsilon^2(q_\perp) / (k_B T)^2} \right]^2 \right] P_{ij}^L(\mathbf{q}_\perp). \quad (3.13)$$

IV. RENORMALIZATION-GROUP TREATMENT OF DISORDER NEAR H_{c1}

Except for the anisotropic gradient couplings, the boson representation (3.9) of flux lines with quenched random impurity disorder resembles a two-component spin model with bond randomness.^{40,41} Although weak disorder produces only small changes far from H_{c1} , quenched impurity fluctuations do become important near the critical point $\mu=0$ of this theory. To determine the relevance of the quenched random fluctuations in $\delta\mu(\mathbf{r}, z)$ (which cause spatial variations in the local H_{c1}), we can use the Harris criterion.⁴¹ Upon adapting arguments used for interacting lines with disorder in two dimensions,⁴² it is easy to show that disorder changes the behavior at H_{c1} provided the specific heat of the *pure* system diverges. Because the specific heat of three-dimensional superconductors without disorder only diverges logarithmically at H_{c1} ,³ we expect that quenched random disorder is a *marginal* operator. As we shall see, this operator is in fact marginally *relevant*, leading eventually to new critical ex-

ponents at sufficiently large length scales near H_{c1} ,²¹ and, possibly, to a new vortex-glass phase.

In this section, we derive the renormalization-group recursion relations for interacting flux lines with weak disorder near H_{c1} , show that disorder is indeed marginally relevant, and estimate the boundary in the (H, T) plane above which the calculations in Sec. III are reliable. We also discuss the current state of the vortex-glass hypothesis.

A. Renormalization-group recursion relations

It is easiest to work in the first quantized representation (3.8), and consider the thermodynamic free energy averaged over disorder,

$$\bar{F} = \overline{\ln Z_N}, \quad (4.1)$$

where the partition function for a fixed configuration of impurities is

$$Z_N = \frac{1}{N!} \prod_{j=1}^N \int \mathcal{D}\mathbf{r}_j(z) e^{-\mathcal{S}_N / k_B T}, \quad (4.2)$$

and \mathcal{S}_N is given by Eq. (3.8). As is often the case with random systems,⁴³ we have found it convenient to use the replica trick. Accordingly, we consider k copies of the partition function (4.2) and obtain the free energy F via the relation

$$F = \lim_{k \rightarrow 0} (\overline{Z}_N^k - 1)/k. \quad (4.3)$$

Upon rewriting the term involving disorder in (3.8) as

$$\sum_{j=1}^N \int dz V_D(\mathbf{r}_j(z), z) \\ = \int d^2r \int dz V_D(\mathbf{r}, z) \sum_{j=1}^N \delta(\mathbf{r} - \mathbf{r}_j(z)), \quad (4.4)$$

and averaging over the distribution of random impurities described by Eq. (3.2), we find that the replicated partition function is

$$\overline{Z}_N^k = \frac{1}{(N!)^k} \prod_{j=1}^N \prod_{\alpha=1}^k \int \mathcal{D}\mathbf{r}_j^\alpha(z) e^{-\mathcal{S}_N/k_B T}, \quad (4.5)$$

with

$$\mathcal{S}_N = \int_0^L dz \left[\frac{\tilde{\epsilon}_1}{2} \sum_{j,\alpha} \left(\frac{d\mathbf{r}_j^\alpha}{dz} \right)^2 + \frac{V_0}{2} \sum_{\alpha} \sum_{i \neq j} \delta(\mathbf{r}_i^\alpha - \mathbf{r}_j^\alpha) \right. \\ \left. - \frac{\Delta}{2k_B T} \sum'_{\substack{i,j \\ \alpha,\beta}} \delta(\mathbf{r}_i^\alpha - \mathbf{r}_j^\beta) \right]. \quad (4.6)$$

The sums over i and j run over N lines, while those over α and β are over k replicas. The prime on the last summation means that it is restricted to the case $(i, \alpha) \neq (j, \beta)$. The self-energy which arises when these pairs of indices are equal has been subtracted out.

As discussed by Kardar for lines with disorder in two dimensions,⁴³ and by M. P. A. Fisher for disordered superconductors,⁵ there is an attractive interaction between different replicas. To determine the consequences of this interaction, we apply the renormalization-group method of Ref. 3. Because the calculations are not very different,

FIG. 5. Interaction vertices for vortex lines with disorder. (a) Repulsive interaction between different lines within the same replica. (b) Attractive interaction between different replicas induced by averaging over the disorder.

we only sketch the main features. There are now two types of interactions between lines, as displayed in Fig. 5. With d dimensions transverse to the flux lines, the two dimensionless coupling constants of the theory are an interaction between identical replicas of two different lines

$$\bar{v} = \frac{V_0 \tilde{\epsilon}_1}{(k_B T)^2} \Lambda^{d-2}, \quad (4.7)$$

as in Ref. 3, and a new coupling constant which measures the strength of the disorder,

$$\bar{\Delta} = \frac{\Delta \tilde{\epsilon}_1}{(k_B T)^3} \Lambda^{d-2}, \quad (4.8)$$

where $\Lambda \sim 1/\lambda$ is the cutoff associated with the Fourier representation of the δ function in Eq. (4.6).³ For simplicity we have assumed a single cutoff in both the δ -function interactions in Eq. (4.6). Fluctuations in the impurity potential on scales shorter than λ can be incorporated into a redefinition of Δ .

The renormalization-group method of Ref. 3 is equivalent to summing up “ladder graphs” which represent the effects of repeated applications of the interactions between vortex lines shown in Fig. 5 (see also Fig. 6). Because the first term in Eq. (4.6) is diagonal in the replica index, the two types of interactions or rungs of the ladders never mix. The renormalization-group recursion relations which result from reducing the cutoff from Λ to Λe^{-l} are very simple. Upon setting $d = 2 - \epsilon$, we have

$$\frac{d\bar{v}}{dl} = \epsilon \bar{v} - K_d \bar{v}^2 \quad (4.9)$$

and

$$\frac{d\bar{\Delta}}{dl} = \epsilon \bar{\Delta} + K_d \bar{\Delta}^2, \quad (4.10)$$

where $K_d = S_d / (2\pi)^d$, and S_d is the surface area of a d -dimensional sphere, $S_d = 2\pi^{d/2} / \Gamma(d/2)$. The recursion relation for \bar{v} is just the result for pure systems.^{32,3} The recursion relation for $\bar{\Delta}$ agrees with the result for a single line wandering in a disordered medium derived by Kar-

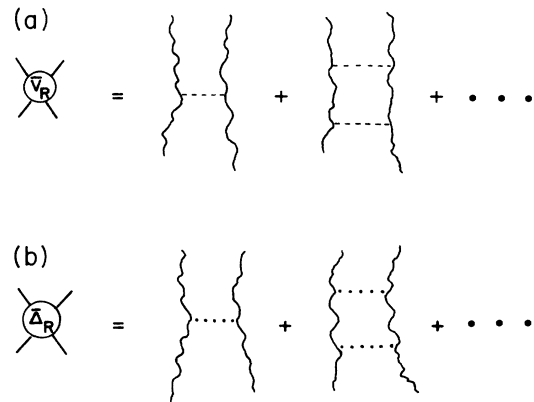


FIG. 6. Ladder graphs which contribute to the renormalized interaction strength \bar{v} , and the renormalized variance of the disorder strength $\bar{\Delta}$.

dar, Parisi, and Zhang.⁴⁴ The disorder is indeed marginally relevant near H_{c1} , even when interactions between lines are taken into account. Note that there is no cross coupling between the interaction coupling constant \bar{v} and the dimensionless disorder strength $\bar{\Delta}$ to this order.

B. Mapping onto the dense limit

The solutions of the recursion relations (4.9) and (4.10) when $d=2$ are

$$\bar{v}(l) = \frac{\bar{v}(0)}{1 + K_2 \bar{v}(0)l} \quad (4.11)$$

and

$$\bar{\Delta}(l) = \frac{\bar{\Delta}(0)}{1 - K_2 \bar{\Delta}(0)l}, \quad (4.12)$$

where $\bar{v}(0)$ and $\bar{\Delta}(0)$ are given by Eqs. (4.7) and (4.8) and $K_2 = 1/2\pi$. Although the disorder grows with increasing length scales according to Eq. (4.12), one can still use these recursion relations to match onto the fluctuation-corrected mean-field theory of Sec. III. To determine when this is possible, we integrate the recursion relations into the dense regime, choosing $l=l^*$ such that³

$$n(l^*)\lambda^2 = e^{2l^*} n_0 \lambda^2 = 1. \quad (4.13)$$

This choice ensures that we are far from the critical point in Eq. (3.9). Calculations like those in Sec. III will then be possible provided $\bar{\Delta}(l^*) \ll 1$. Disorder will dominate the physics, however, if $\bar{\Delta}(l^*) = O(1)$. Upon inserting Eq. (4.13) into (4.12), we see that this will happen for flux-line densities such that

$$n_0 \lambda^2 \lesssim e^{-4\pi/\bar{\Delta}}, \quad (4.14)$$

which is equivalent to the criterion (1.4) discussed in the Introduction.⁴⁵ The thermal fluctuations which lead to entanglement will screen out the disorder whenever

$$n_0 \lambda^2 \gg e^{-4\pi/\bar{\Delta}}, \quad (4.15)$$

which is equivalent to Eq. (1.5). When this inequality is satisfied, we can obtain the structure function by matching onto the weak disorder results of Sec. III via a relation like that used in Ref. 3,

$$S(q_\perp, q_z, \bar{v}, \bar{\Delta}) = S(e^{l^*} q_\perp, e^{2l^*} q_z, \bar{v}(l^*), \bar{\Delta}(l^*)). \quad (4.16)$$

For a discussion of screening of disorder in bosons where $V_D(\mathbf{r}, z)$ is independent of z (the issue here is boson localization), see Ref. 46.

C. Is there a vortex-glass transition?

Upon using the constitutive relation between $B = n\phi_0$ and H derived for pure systems in Ref. 3,

$$B(H) = \frac{\bar{v}}{4\pi} (H - H_{c1}) \ln \left[\frac{4\pi}{\bar{v}} \frac{(\phi_0/\lambda^2)}{H - H_{c1}} \right], \quad (4.17)$$

we see that Eq. (4.14) defines a line $H_d(T)$ in the (H, T) plane, below which disorder produces new physics, given by the solution of

$$(H_d - H_{c1}) \ln \left[\frac{4\pi}{\bar{v}} \frac{(\phi_0/\lambda^2)}{H_d - H_{c1}} \right] = \frac{4\pi\phi_0}{\bar{v}\lambda^2} e^{-4\pi(k_B T)^3/\bar{\epsilon}_1 \Delta}. \quad (4.18)$$

Note that $\phi_0/\lambda^2 = O(H_{c1})$, so that $(H_d - H_{c1})/H_{c1} \lesssim 4\pi/\bar{v}$. Because \bar{v} is so large [$\bar{v} = O(10^5)$], the disorder-dominated regime is actually much smaller than shown in Fig. 1(b). Because $\bar{\epsilon}_1$ vanishes as $T \rightarrow T_c$, the region of Fig. 1(b) dominated by disorder shrinks to zero in this limit.

Is this disorder-dominated region a ‘‘vortex glass,’’⁵ or does it simply represent a crossover to new critical exponents at H_{c1} ? A phenomenological theory of the constitutive relation which replaces Eq. (4.17) in this region has been worked out by Natterman and Lipowsky,²¹ based on the properties a *single* line in a disordered medium. Although the instability summarized by Eq. (4.10) has so far precluded an analytic treatment, there is numerical evidence that a single line wanders according to⁴⁴

$$\overline{|\mathbf{r}(z) - \mathbf{r}(0)|^2} \sim |z|^{2\nu}, \quad (4.19)$$

with $\nu \approx 0.6$. Natterman and Lipowsky show that this leads to²¹

$$B(H) \sim (H - H_{c1})^{\bar{\beta}}, \quad (4.20)$$

with $\bar{\beta} = \nu/(1-\nu) \approx 1.5$. These results are presumably correct even if a vortex-glass-phase transition occurs somewhere above H_{c1} .

M. P. A. Fisher gives several arguments for a thermodynamically distinct vortex-glass phase.⁵ He shows, in particular, that a model of interacting lines with disorder in two dimensions leads to a renormalization-group instability which he interprets as evidence for a vortex-glass-phase transition. He then argues that such a transition is therefore even *more* likely to occur in three dimensions. Edge dislocations,⁴⁷ however, are excluded from Fisher’s two-dimensional model. Such dislocations could allow for a *gradual* transition from a dilute region where disorder dominates, to a dense liquid of lines where disorder is a small perturbation.⁴⁸ Although it is sensible to exclude dislocations for lines which cannot start or stop inside a medium in two dimensions, these defects are *inevitable* in three-dimensional vortex liquids for topological reasons. As discussed in Ref. 22, the relevant dislocations have a mixed edge and screw character, and do not require that vortex lines stop or start inside the medium. It is hard to rule out a gradual transition from a dilute disorder-dominated regime to a dense thermally dominated liquid regime (possibly mediated by disclinations as well) under these conditions.

There is numerical evidence that the disorder-induced instability in dilute two-dimensional vortex lines does indeed lead to glassy behavior.⁴⁹ In the absence of convincing numerical work, the interpretation of instabilities as transitions to new phases of matter should be viewed with caution. There is, for example, a similar instability at low temperatures in a soluble gauge glass model in two dimensions.⁵⁰ Here, however, the instability merely leads to a *reentrant* disordered phase which is *continuously connected* to a liquidlike high-temperature regime. There is

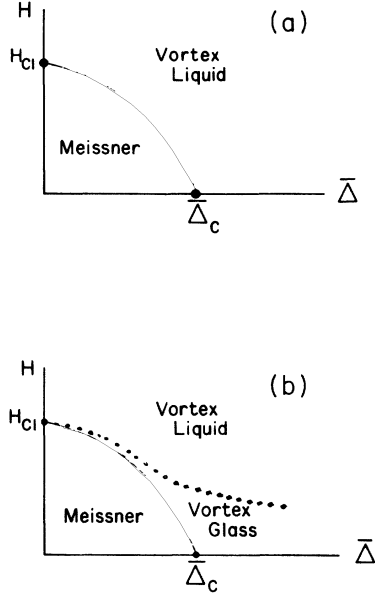


FIG. 7. Two possible phase diagrams for vortex liquids at high temperatures in the presence of disorder. In (a), disorder simply leads to a suppression of H_{c1} and new critical exponents along the line $H_{c1}(\bar{\Delta})$ for $\bar{\Delta} \neq 0$. Although a single vortex line may exhibit glassy behavior (Ref. 52), the vortex-glass “phase” in this scenario exists only in the limit of infinite dilution along the line $H_{c1}(\bar{\Delta})$ itself. In (b), there is a true vortex-glass phase, extending a finite distance above H_{c1} for all nonzero $\bar{\Delta}$.

no true vortex glass, except possibly at zero temperature. The gauge glass model has recently been studied numerically in *three* dimensions by Huse and Seung,⁵¹ who find evidence which slightly favors the vortex-glass hypothesis. A recent analysis of ϵ -expansion results for the gauge glass by Moore and Murphy, however, suggests that the lower critical dimension for spin-glass order is in fact *greater* than three.⁵² Although results on the statistical mechanics of a single vortex line can be interpreted in terms of spin-glass behavior⁵³ (described by a zero-temperature fixed point), this would convincingly establish the existence of a vortex-glass phase only *on* the H_{c1} line itself, and not above this line.

The best evidence for the vortex-glass hypothesis at present is probably the striking phenomenological fit obtained using these ideas to the experiments of Koch *et al.*⁶ Figure 7 shows two possible phase diagrams at fixed temperature, as a function of field and disorder strength, close to H_{c1} . Further analytic or numerical work which shows which (if any), of these diagrams is correct would be most welcome.

ACKNOWLEDGMENTS

We would like to acknowledge stimulating interactions with C. Marchetti, especially (D.R.N.) during the early stages of this investigation. We would also like to thank D.S. Fisher for helpful conversations and a critical reading of the manuscript. This work was supported by the

National Science Foundation, through Grant No. DMR 88-17291 and through the Harvard Materials Research Laboratory.

APPENDIX A: CONNECTION BETWEEN MAGNETIC-FIELD FLUCTUATIONS AND VORTEX CONFIGURATIONS

The magnetic-field fluctuations at length scales much larger than the London length λ are locked to the fluctuations in the vortex positions. Here, we use the London equation to estimate magnetic-field correlations over a broader range of length scales, down to the coherence length $\xi \ll \lambda$. For simplicity, we restrict our discussion to pure (i.e., nonrandom) systems.

For isotropic superconductors permeated by a set of vortex lines described by (1.2) and (1.3), the London equation reads

$$\mathbf{b}(\mathbf{r}, z) - \lambda^2 \nabla^2 \mathbf{b}(\mathbf{r}, z) = \phi_0 \mathbf{T}(\mathbf{r}, z), \quad (\text{A1})$$

where the vortex “currents” $T_z = n(\mathbf{r}, z)$, $\mathbf{T}_\perp = \mathbf{t}(\mathbf{r}, z)$ act as source terms. For a given position of the flux lines $\{\mathbf{r}_i(z)\}$ the corresponding magnetic field can be obtained using (A1). From this equation one deduces

$$\langle \delta b_\mu(\mathbf{q}) \delta b_\nu(-\mathbf{q}) \rangle = \frac{\phi_0^2}{(1 + \lambda^2 q^2)^2} \langle T_\mu(\mathbf{q}) T_\nu(-\mathbf{q}) \rangle, \quad (\text{A2})$$

which leads to Eqs. (2.9) and (2.10).

It is straightforward to generalize this approach to an anisotropic superconductor with a (dimensionless) diagonal mass tensor [with $(\mathbf{r}, z) = (x, y, z) \equiv x_\mu$] $m_{xx} = m_{yy} = m_\perp$, $m_{zz} = m_z$. The London equation now reads⁵⁴

$$b_\mu - \lambda^2 m_{\sigma\tau} \epsilon_{\tau\alpha\mu} \epsilon_{\sigma\beta\nu} \frac{\partial^2 b_\nu}{\partial x_\alpha \partial x_\beta} = \phi_0 T_\mu, \quad (\text{A3})$$

where $\epsilon_{\alpha\beta\gamma}$ is the Levi-Civita antisymmetric tensor. We use the notation of Kogan.⁵⁴ Equation (A3) is readily inverted in Fourier space, and leads to the following relations between b and \mathbf{T} :

$$b_z(\mathbf{q}) = \frac{\phi_0}{1 + \lambda^2 m_\perp q^2} n(\mathbf{q}), \quad (\text{A4})$$

$$b_{i1}(\mathbf{q}) = \frac{\phi_0}{1 + \lambda^2 (m_z q_1^2 + m_\perp q_z^2)} P_{ij}^T(\mathbf{q}_1) t_j(\mathbf{q}) + \frac{\phi_0}{1 + \lambda^2 m_\perp q^2} P_{ij}^L(\mathbf{q}_1) t_j(\mathbf{q}). \quad (\text{A5})$$

One now readily obtains

$$\langle \delta b_z(\mathbf{q}) \delta b_z(-\mathbf{q}) \rangle = \frac{\phi_0^2}{(1 + \lambda^2 m_\perp q^2)^2} S(\mathbf{q}_1, q_z), \quad (\text{A6})$$

$$\begin{aligned} \langle \delta b_{\perp,i}(\mathbf{q}) \delta b_{\perp,j}(-\mathbf{q}) \rangle &= \frac{\phi_0^2}{(1+\lambda^2 m_{\perp} q^2)^2} P_{ij}^L(\mathbf{q}_{\perp}) A(\mathbf{q}_{\perp}, q_z) \\ &+ \frac{\phi_0^2}{[1+\lambda^2(m_z q_1^2 + m_{\perp} q_z^2)]^2} \\ &\quad \times P_{ij}^T(\mathbf{q}_{\perp}) B(\mathbf{q}_{\perp}, q_z), \end{aligned} \quad (\text{A7})$$

where $A(\mathbf{q}_{\perp}, q_z)$ and $B(\mathbf{q}_{\perp}, q_z)$ are the longitudinal and transverse parts of the tangent correlation function defined in Eq. (2.26).

The above formulas are only a zeroth order estimate. Indeed, for a given configuration of vortices $\{\mathbf{r}_i(z)\}$ one has

$$\mathbf{b} = \mathbf{b}_{\text{London}}(\{\mathbf{r}_i(z)\}) + \delta \mathbf{b}', \quad (\text{A8})$$

where $\mathbf{b}_{\text{London}}$ is the saddle-point solution of minimization of the Landau-Ginsburg free energy for fixed vortex positions. $\delta \mathbf{b}'$ represents thermal deviations from the solution of the London equation. Thus, up to now, only magnetic-field extrema associated with a fixed set of vortex positions have been taken into account in the calculation of the fluctuations. One can, however, estimate the effect of these additional terms. Within the London theory, the above correlation functions simply acquire

the additional terms,

$$\langle \delta b'_z(\mathbf{q}) \delta b'_z(-\mathbf{q}) \rangle = 4\pi k_B T \frac{\lambda^2 m_{\perp} q_1^2}{1+\lambda^2 m_{\perp} q^2}, \quad (\text{A9})$$

$$\begin{aligned} \langle \delta b'_{\perp,i}(\mathbf{q}) \delta b'_{\perp,j}(-\mathbf{q}) \rangle &= 4\pi k_B T \left[\frac{\lambda^2 m_{\perp} q_z^2}{1+\lambda^2 m_{\perp} q^2} P_{ij}^L(\mathbf{q}_{\perp}) \right. \\ &\quad \left. + \frac{\lambda^2 m_{\perp} m_z q^4}{\lambda^2 m_{\perp} m_z q^4 + m_{\perp} q_1^2 + m_z q_z^2} P_{ij}^T(\mathbf{q}_{\perp}) \right], \end{aligned} \quad (\text{A10})$$

obtained from the term quadratic in the fields in the London free energy,

$$F_L = \int dz dr \frac{1}{8\pi} (b^2 + \lambda^{-2} m_{ij}^{-1} A_i A_j). \quad (\text{A11})$$

Here, we set $\mathbf{b} = \nabla \times \mathbf{A}$ and work in the gauge $\nabla \cdot \mathbf{A} = 0$.

Disorder on short length scales will also modify the above results. We have not attempted to estimate this effect.

APPENDIX B: CORRELATION FUNCTIONS USING REPLICAS

In this appendix we show that the result (3.12) for the structure function in presence of weak disorder can also be obtained by applying the replica method to the coherent states path-integral representation associated with (3.9). The replica method allows us to compute averages of the type

$$C(\mathbf{r}, z) = \overline{\langle n(\mathbf{r}, z) n(0, 0) \rangle} - \overline{\langle n(\mathbf{r}, z) \rangle} \overline{\langle n(0, 0) \rangle} \quad (\text{B1})$$

through

$$C(\mathbf{r}, z) = \lim_{m \rightarrow 0} \frac{1}{m} \sum_{\alpha=1}^m \langle n_{\alpha}(\mathbf{r}, z) n_{\alpha}(0, 0) \rangle_c, \quad (\text{B2})$$

where a set of m replicated fields have been introduced, $\langle \rangle_c$ is the connected part of the thermal average, and the overbar denotes an average over the disorder. One can explicitly separate in (3.12) the contributions to the averaged structure function due to thermal fluctuations and to disorder, respectively, by writing $C(r, z) = C_{th}(r, z) + C_D(r, z)$ with

$$C_{th}(r, z) = \overline{\langle n(r, z) n(0, 0) \rangle} - \overline{\langle n(r, z) \rangle} \overline{\langle n(0, 0) \rangle}$$

and

$$C_D(r, z) = \langle n(r, z) \rangle \langle n(0, 0) \rangle - n_0^2.$$

Note that in a scattering experiment it is the sum $C(r, z)$ which is measured.

The above correlation functions are associated with the replicated grand canonical partition function:

$$\overline{Z_g^m} = \int \prod_{\alpha=1}^m \mathcal{D}\psi_{\alpha}^* \mathcal{D}\psi_{\alpha} \exp \left[- \sum_{\alpha=1}^m S(\psi_{\alpha}^*, \psi_{\alpha}) / k_B T \right] \equiv \int \prod_{\alpha=1}^m \mathcal{D}\psi_{\alpha}^* \mathcal{D}\psi_{\alpha} \exp \left[- \tilde{S}(\psi_{\alpha}^*, \psi_{\alpha}) / k_B T \right], \quad (\text{B3})$$

where $S(\psi^*, \psi)$ has been defined in (3.9). The replicated action reads

$$\tilde{S} = \int dz dr \left[\sum_{\alpha} \left[in_{\alpha} k_B T \frac{\partial \theta_{\alpha}}{\partial z} + \frac{(k_B T)^2}{8\tilde{\epsilon}_1 n_{\alpha}} (\nabla n_{\alpha})^2 + \frac{(k_B T)^2 n_{\alpha}}{2\epsilon_1} (\nabla \theta_{\alpha})^2 + \frac{V_0}{2} n_{\alpha}^2 - \mu n_{\alpha} \right] - \frac{\Delta}{2k_B T} \sum_{\alpha, \beta} n_{\alpha} n_{\beta} \right]. \quad (\text{B4})$$

Let us first examine the mean-field solution with constant density. It is minimized for $n_{\alpha} = n_0(m)$, where $n_0(m)$ minimizes the mean-field Lagrangian,

$$\tilde{\mathcal{L}}_{\text{MFT}} = m \left[-\mu n_0 + \left[\frac{V_0}{2} - m \frac{\Delta}{2k_B T} \right] n_0^2 \right], \quad (\text{B5})$$

i.e., $n_0(m) = \mu / (V_0 - m\Delta/k_B T)$. The action becomes unbounded for $m > m_c = k_B T V_0 / \Delta$, but this is an artifact of the model. The problem is only that moments $\overline{Z^m}$ do not exist for m too large for a model with a Gaussian distribution. To see that this singular behavior is harmless, let us look at the simple integral

$$Z(\delta\mu) = \int_{-\infty}^{+\infty} dx \exp \left[\frac{1}{k_B T} \left(\mu x - \frac{V_0}{2} x^2 \right) + \frac{\delta\mu}{k_B T} x \right] = C \exp \left[\frac{(\mu + \delta\mu)^2}{2k_B T V_0} \right], \quad (\text{B6})$$

with $C = (2\pi k_B T / V_0)^{1/2}$. Now if $\delta\mu$ is distributed according to a centered Gaussian of variance Δ , clearly Z^m is infinite for $m > m_c$. However, $\ln Z = \ln C + (\mu^2 + \Delta) / (2TV_0)$ is well defined, and it is a simple exercise to check that it is given by the limit for $m \rightarrow 0$ of the expression $(Z^m - 1) / m$ computed via the replica trick for $m < m_c$. For the model (B4) the same artifact occurs and can be removed either by considering better behaved randomness or higher-order terms in the density expansion. We thus assume everywhere $m < m_c$.

For fixed m , the action (B4) can be expanded in $\pi_\alpha = n_\alpha - n_0(m)$ and $\nabla\theta_\alpha$ to quadratic order. Upon introducing a set of vectors $X_\alpha = \begin{pmatrix} \theta_\alpha \\ \pi_\alpha \end{pmatrix}$ it is easy to see that the matrix of the quadratic form takes the cyclic form

$$G^{-1} = \begin{bmatrix} A & B & \cdots & B \\ B & A & \cdots & B \\ \vdots & \vdots & \ddots & \vdots \\ B & B & \cdots & A \end{bmatrix}, \quad (\text{B7})$$

where A and B are 2×2 matrices:

$$A = \begin{bmatrix} \frac{q_1^2 n_0 (k_B T)^2}{\bar{\epsilon}_1} & -q_z k_B T \\ q_z k_B T & V_0 + \frac{(k_B T)^2 q_1^2}{8\bar{\epsilon}_1 n_0} - \frac{\Delta}{k_B T} \end{bmatrix}, \quad B = \begin{bmatrix} 0 & 0 \\ 0 & -\frac{\Delta}{k_B T} \end{bmatrix}. \quad (\text{B8})$$

Defining $Y_\alpha = \sum_{\alpha=1}^m \exp[2\pi i \alpha (\alpha/m)] X_\alpha$ for $\alpha = 0, \dots, m-1$ puts G^{-1} into block diagonal form, with one mode $Y_0 = \sum_\alpha X_\alpha$ associated with the matrix A_1

$$A_1 = \begin{bmatrix} \frac{q_1^2 n_0 (k_B T)^2}{\bar{\epsilon}_1} & -q_z k_B T \\ q_z k_B T & V_0 + \frac{(k_B T)^2 q_1^2}{8\bar{\epsilon}_1 n_0} - \frac{\Delta}{k_B T} \end{bmatrix} \quad (\text{B9})$$

and the $(m-1)$ other modes associated with the matrix A_0 of the pure system defined in (2.25). Upon using the formula $\sum_\alpha \exp[2\pi i \alpha (\alpha/m)] \exp(2\pi i \alpha \beta / m) = m \delta_{\alpha\beta}$, one finds

$$\begin{aligned} \overline{\langle \pi(\mathbf{q}) \pi(\mathbf{q}) \rangle} &= \lim_{m \rightarrow 0} \frac{1}{m} \sum_{\alpha \leq 1}^m \langle \pi_\alpha(\mathbf{q}) \pi_\alpha(-\mathbf{q}) \rangle \\ &= \lim_{m \rightarrow 0} \frac{1}{m} \left[(m-1) \frac{n_0 q_1^2 k_B T / \bar{\epsilon}_1}{q_z^2 + \epsilon^2(q_1) / (k_B T)^2} + \frac{n_0 q_1^2 k_B T / \bar{\epsilon}_1}{q_z^2 + \epsilon^2(q_1) / (k_B T)^2 - m(\Delta/k_B T) n_0 (q_1^2 / \bar{\epsilon}_1)} \right]. \quad (\text{B10}) \end{aligned}$$

After taking the limit $m \rightarrow 0$ explicitly, we find a result for $\overline{S(\mathbf{q}, q_z)} = \overline{\langle \pi(\mathbf{q}) \pi(-\mathbf{q}) \rangle}$, which agrees with Eq. (3.12). The matrix G^{-1} in (B7) is easily inverted. In the limit $m \rightarrow 0$ one obtains both correlations diagonal and off-diagonal in replicas in terms of the vector x_α introduced above ($i = 1, 2, j = 1, 2, \alpha \neq \beta$):

$$\langle x_{\alpha i} x_{\alpha j} \rangle = (A_0^{-1} - A_0^{-1} B A_0^{-1})_{ij}, \quad \langle x_{\alpha i} x_{\beta j} \rangle = -(A_0^{-1} B A_0^{-1})_{ij}$$

from which one sees that the thermal part $C_{\text{th}}(r, z)$ is unchanged by disorder (in mean field):

$$C_{\text{th}}(\mathbf{q}) = \lim_{m \rightarrow 0} \{ \langle \pi_\alpha(\bar{q}) \pi_\alpha^*(\bar{q}) \rangle - \langle \pi_\alpha(\mathbf{q}) \pi_\beta^*(\bar{q}) \rangle \} = C_{\text{th}}(\bar{q}, \Delta = 0).$$

*Also at Laboratoire de Physique Théorique (ENS), Laboratoire propre du CNRS associé à l'École Normale Supérieure et à l'Université de Paris-Sud.

¹P. L. Gammel, D. J. Bishop, G. J. Dolan, J. R. Kwo, C. A.

Murray, L. F. Schneemeyer, and J. V. Waszczak, Phys. Rev. Lett. **59**, 2592 (1987).

²A. P. Malozemoff, T. K. Worthington, Y. Yeshurun, and F. Holtzberg, Phys. Rev. B **38**, 7203 (1988), and references

- therein.
- ³D. R. Nelson, Phys. Rev. Lett. **69**, 1973 (1988); D. R. Nelson and S. Seung, Phys. Rev. B **39**, 9153 (1989); D. R. Nelson, J. Stat. Phys. **57**, 511 (1989).
- ⁴P.L. Gammel, L. F. Schneemeyer, J. V. Waszczak, and D. J. Bishop, Phys. Rev. Lett. **61**, 1666 (1988).
- ⁵M. P. A. Fisher, Phys. Rev. Lett. **62**, 1415 (1989); D. Fisher, M. P. A. Fisher, and D. Huse, Phys. Rev. B (to be published). For earlier work on the vortex-glass state, see S. John and T. C. Lubensky, *ibid.* **34**, 4815 (1986).
- ⁶R. H. Koch *et al.*, Phys. Rev. Lett. **63**, 1511 (1989). There is still some debate about the evidence cited for a vortex-glass-phase transition in this paper; see S. N. Coppersmith, M. Inui, and P. G. Littlewood, Phys. Rev. Lett. **64**, 2585 (1990); R. H. Koch, V. Foglietti, and M. P. A. Fisher, *ibid.* **64**, 2586 (1990).
- ⁷T. K. Worthington, F. H. Holtzberg, and C. A. Feild, Cryogenics **30**, 417 (1990).
- ⁸A. Houghton, R. A. Pelcovits, and A. Sudbo, Phys. Rev. B **40**, 6763 (1989).
- ⁹G. J. Dolan, G. V. Chandrasekar, T. R. Dinger, C. A. Feild, and F. Holtzberg, Phys. Rev. Lett. **62**, 827 (1989).
- ¹⁰E. H. Brandt, P. Esquinazi, and G. Wiess, Phys. Rev. Lett. **62**, 827 (1989).
- ¹¹C. Marchetti and D. R. Nelson, Phys. Rev. B **42**, 9938 (1990).
- ¹²As pointed out in Ref. 5, a description in terms of decoupled planes of point vortices may in fact be appropriate in Ba-Sr-Ca-Cu-O when $H \gtrsim 1$ T due to the exceptionally weak interplanar couplings in these materials. The only source of a large liquid viscosity in this case is collective effects associated with two-dimensional melting. Similar conclusions have been reached by V. M. Vinokar, P. H. Kes, and A. E. Koshelev, Physica C (to be published) and by L. Glazman (unpublished). Vortex lines degenerate into decoupled planes when thermal fluctuations cause an individual line to jump a distance comparable to an intervortex spacing when passing from one CuO₂ plane to the next. This happens only for $H \gtrsim 50$ T in Y-Ba-Cu-O. Although melting temperatures extracted from the theory of two-dimensional melting are probably accurate in this regime, correlations in the crystalline phase are *never* two-dimensional in the asymptotic long-wavelength limit. The presence of any nonzero interplanar coupling leads, in particular, to *three*-dimensional δ -function Bragg peaks (with anisotropic diffuse scattering) at all temperatures below the melting point. See B. J. Birgeneau and D. J. Litster, J. Phys. Lett. (Paris) **39**, L399 (1978).
- ¹³S. Obukhov and M. Rubinstein, Phys. Rev. Lett. **65**, 1279 (1990).
- ¹⁴See, e.g., the articles by A. L. Fetter and P. C. Hohenberg, by Y. B. Kim and M. J. Stephen, and by W. F. Vinen, in *Superconductivity*, edited by R. D. Park (Marcel Dekker, New York, 1969), Vol. 2.
- ¹⁵Remarkably, there do not yet appear to be decoration experiments which compare the configuration of flux lines which enters a sample with that which emerges from the other side.
- ¹⁶E. M. Forgan, D. McK. Paul, H. A. Mook, P. A. Timmins, H. Keller, S. Sutton, and J. S. Abell, Nature (London) **343**, 735 (1990).
- ¹⁷D. Cribier, B. Jacrot, L. M. Rao, and B. Farnoux, Phys. Rev. Lett. **9**, 106 (1966).
- ¹⁸D. K. Christen, F. Tasset, S. Spooner, and J. A. Mook, Phys. Rev. B **15**, 4506 (1977).
- ¹⁹For an illustration of how flux-line motion begins to blur conventional decoration photographs with increasing temperature, see R. N. Kleiman, P. L. Gammel, L. F. Schneemeyer, J. V. Waszczak, and D. J. Bishop, Phys. Rev. Lett. **62**, 827 (1989).
- ²⁰E. H. Brandt, Phys. Rev. B **34**, 6514 (1986); Phys. Rev. Lett. **63**, 1106 (1989).
- ²¹T. Natterman and R. Lipowsky, Phys. Rev. Lett. **61**, 2508 (1988).
- ²²M. C. Marchetti and D. R. Nelson, Phys. Rev. B **41**, 1910 (1990). The dislocation-mediated melting hypothesis explored here is also applicable via the boson analogy of Ref. 3 to quantum melting of two-dimensional boson crystals at zero temperature. Little is known about the hexatic superfluid phase predicted by this approach.
- ²³E. M. Chudnovsky, Phys. Rev. B **40**, 11355 (1990); and (unpublished).
- ²⁴C. A. Murray, P. L. Gammel, D. J. Bishop, D. B. Mitzi, and A. Kapitulnik, Phys. Rev. Lett. **64**, 2312 (1990).
- ²⁵A. I. Larkin and Yu. N. Ovchinnikov, J. Low Temp. Phys. **34**, 409 (1979).
- ²⁶P. Le Doussal and D. R. Nelson (unpublished).
- ²⁷See, e.g., J. W. Negele and J. Orland, *Quantum Many-Particle Systems* (Addison-Wesley, New York, 1988), Chaps. 1 and 2.
- ²⁸V. N. Popov, *Functional Integrals and Collective Excitations* (Cambridge University Press, New York, 1987).
- ²⁹G. D. Mahan, *Many-Particle Physics* (Plenum, New York, 1981).
- ³⁰P. G. de Gennes and J. Matricon, Rev. Mod. Phys. **36**, 45 (1964).
- ³¹See A. A. Abrikosov, L. P. Gorkov, and I. E. Dzyaloshinski, *Methods of Quantum Field Theory in Statistical Physics* (Prentice-Hall, Englewood Cliffs, NJ, 1963).
- ³²First worked out two-dimensional superfluids by V. N. Popov in Theor. Math. Phys. **11**, 565 (1972), and rederived using renormalization-group techniques by D. S. Fisher and P. C. Hohenberg, Phys. Rev. B **37**, 4936 (1988). A renormalization-group derivation with the free boundary conditions appropriate for vortex lines is given in Ref. 3.
- ³³R. P. Feynman, *Statistical Mechanics* (Benjamin, Reading, MA, 1972).
- ³⁴One might also hope to use the Bogoliubov approximation corrected in this way to model the structure function of flux liquids which are sufficiently dense so that $n_0 \lambda^2 \gg 1$. In this limit, each vortex sits in an approximately constant potential due to interactions with many distant neighbors. The most important interaction between neighboring vortices is then a hard-core repulsion which sets in at the coherence length $\xi \ll \lambda$. An approximate effective potential in this limit would take the form (2.17), where the cutoff implicit in the δ function is ξ instead of λ .
- ³⁵P. G. de Gennes, Mol. Cryst. Liq. Cryst. **34**, 177 (1977).
- ³⁶J. V. Selinger and R. F. Bruinsma (unpublished).
- ³⁷E. H. Brandt, Phys. Rev. B **34**, 6514 (1986).
- ³⁸D. R. Nelson, in *Phase Transitions and Critical Phenomena*, edited by C. Domb and J. L. Lebowitz (Academic, New York, 1983), Vol. 7.
- ³⁹Disorder due to a frozen distribution of grain or twin boundaries is qualitatively different, except possibly on scales much larger than the boundary spacing. The randomness is *correlated* by the planar nature of the disorder in this case.
- ⁴⁰See, e.g., T. C. Lubensky in *III-Condensed Matter*, edited by R. Balian, R. Maynard, and G. Toulouse (North-Holland, New York, 1979).

- ⁴¹A. B. Harris, *J. Phys. C* **7**, 1671 (1974).
- ⁴²M. Kardar and D. R. Nelson, *Phys. Rev. Lett.* **55**, 1157 (1985).
- ⁴³M. Kardar, *Nucl. Phys. B* **290**, 582 (1987).
- ⁴⁴M. Kardar, G. Parisi, and Y.-C. Zhang, *Phys. Rev. Lett.* **56**, 889 (1986); Kardar and Y.-C. Zhang, *ibid.* **58**, 2087 (1987).
- ⁴⁵A related crossover criterion for the behavior of critical currents can be inferred from the paper of M. B. Feigelman and V. M. Vinokur, *Phys. Rev. B* **41**, 8986 (1990). Their formula for the critical current at high temperatures and low fields, in particular, has an exponential factor that is similar to the right-hand side of Eq. (1.4).
- ⁴⁶M. P. A. Fisher, P. B. Weichman, G. Grinstein, and D. S. Fisher, *Phys. Rev. B* **40**, 546 (1989); D. K. K. Lee and J. M. F. Gunn (unpublished).
- ⁴⁷See, e.g., S. N. Coopersmith, D. S. Fisher, B. I. Halperin, P. A. Lee, and W. F. Brinkman, *Phys. Rev. B* **25**, 349 (1982).
- ⁴⁸This is precisely what happens in crystalline and fluid films on a substrate with a random topography. See S. Sachder and D. R. Nelson, *J. Phys. C* **17**, 5473 (1984).
- ⁴⁹M. P. A. Fisher (private communication).
- ⁵⁰M. Rubinstein, B. Shraiman, and D. R. Nelson, *Phys. Rev. B* **27**, 1800 (1983).
- ⁵¹D. Huse and H. S. Seung, *Phys. Rev. B* **42**, 1059 (1990).
- ⁵²M. A. Moore and M. Murphy (unpublished).
- ⁵³M. Mezard, *J. Phys. (Paris)* **51**, 1831 (1990), and references therein.
- ⁵⁴V. G. Kogan, *Phys. Rev. B* **24**, 1572 (1981).